microplastics

MDPI

Article

Transport of (Micro)plastic Within a River Cross-Section—Spatio-Temporal Variations and Loads

Peter Chifflard [1,2,*], Thorsten Nather [1,3] and Collin J. Weber [1,4]

[1] Department of Geography, Philipps-University Marburg, Deutschhausstraße 10, 35037 Marburg, Germany; weber@geo.tu-darmstadt.de (C.J.W.)
[2] Kompetenzzentrum Wasser Hessen, Max-von-Laue-Straße 13, 60438 Frankfurt am Main, Germany
[3] Engineering Office Greiwe and Helfmeier, 59302 Oelde, Germany
[4] Institute for Applied Geosciences, Technical University Darmstadt, 64287 Darmstadt, Germany
* Correspondence: peter.chifflard@geo.uni-marburg.de; Tel.: +49-6421-28-24155

Abstract: Despite substantial research, the spatio-temporal dynamics of microplastic fluxes remain underexplored, especially in lower-order rivers. This study aims to quantify microplastic loads using a spatio-temporal sampling approach in a single cross-section of the Lahn River, a typical low-mountain river in Central Germany, over a sampling period from July 2020 to April 2021, covering varying discharge conditions, from low to high flow. A total of 198 plastic particles were detected, averaging 3.67 particles per hour, with a mean microplastic load of 0.03 ± 0.027 particles per cubic metre. Microplastic abundance varied spatially within the river cross-section, with lower concentrations found at deeper sampling positions. The data indicate that higher discharge conditions correlate with increased microplastic loads, predominantly at the water surface, suggesting that hydrological conditions significantly influence plastic transport dynamics. However, it remains unclear whether the microplastics observed at higher discharges originate from additional sources or are reactivated from river sediments. This research highlights the need for further studies to validate model assumptions and better understand the reactivation and transport mechanisms of microplastics in river systems.

Keywords: microplastics; hydrology; Lahn River; fluvial transport; flood; low flow

Citation: Chifflard, P.; Nather, T.; Weber, C.J. Transport of (Micro)plastic Within a River Cross-Section—Spatio-Temporal Variations and Loads. *Microplastics* **2024**, *3*, 755–770. https://doi.org/10.3390/microplastics3040047

Academic Editor: Nicolas Kalogerakis

Received: 10 September 2024
Revised: 22 November 2024
Accepted: 3 December 2024
Published: 16 December 2024

1. Introduction

Plastics have become ubiquitous in all kinds of environmental systems worldwide. The ongoing global plastic crisis further contributes to plastic leaking into the environment and being retained there [1]. The plastic residues present in the environment can be defined as human-made, polymeric, and solid particles often classified according their size during production or after fragmentation by biogeochemical and physical processes in the environment [2,3]. In particular, microplastic particles, defined as large microplastics (5000–1000 µm) and microplastics (1000–1 µm) in contrast to macro- (>5000 µm) or nanoplastics (<1 µm) [4], are often considered because their small size allows them to reach a wide spatial distribution and cause a wide variety of environmental risks [5]. Since the exponential increase in global plastic production since the 1950s, both plastics in general and microplastics consist mainly of thermoplastics, with different polyethylenes (PEs) or polypropylenes (PPs) as the most common ones [6]. Combined with numerous additives, occurring in different sizes and shapes, they pose a major threat to the global environment [7–9].

Among other ecosystems, freshwater systems are particularly affected by microplastics as they act as major transport corridors of plastic residues through the environment [7,10]. Research performed over the years has demonstrated that microplastics are present within freshwater systems including water, sediments, and biota [5,11,12]. Furthermore, microplastics can be transported via freshwater systems over long distances, contributing to marine

plastic pollution [13]. However, not only transport but also temporal deposition occurs in freshwater systems [14–16]. Thus, microplastic particles can sink in the water column and be temporally deposited in bed sediments [15,17] but also on embankments [18] and surrounding floodplains [19]. Microplastic particles exhibit varying transport and retention behaviours in water, influenced by their density and shape [20]. While many polymers are buoyant due to their low density, others, like polyvinyl chloride (PVC), polyethylene terephthalate (PET), and nylon, are denser than water and tend to sink naturally. Additionally, as biofouling, such as microalgae growth, increases particle density, even lighter plastics can accumulate in sediments over time. Particle shape also affects retention, with irregularly shaped particles having more complex settling patterns compared to spherical ones [21]. Buoyant particles with irregular forms are more likely to be submerged and trapped underwater than to return to the surface. Studies have shown that larger microplastics tend to stay within riverbed sediments more persistently, though shape may be a more critical factor than size for certain retention patterns. However, the transport and sedimentation of plastic particles show large temporal and spatial variations. Although discharge and flow conditions are known to be important factors, the transport mechanisms have not been fully elucidated, as the characteristics of the plastic particles play an important role. Together, these factors illustrate the complexity in modelling microplastic behaviour within river systems [20].

As freshwater systems are highly dynamic environmental systems, different environmental and anthropogenic drivers affect microplastic input, transport, and deposition within those system. Thus, dependencies of microplastic loads on land use and population density in surrounding and catchment areas have been previously found [16,22]. Furthermore, a combination of point sources (e.g., WWTPs, urban discharge) and diffuse sources (e.g., atmospheric deposition, littering) contribute to the microplastic contamination of freshwaters [14,23]. Finally, recent research demonstrated that microplastic particles behave differently within freshwater depending on their size, shape, polymeric composition, or surface degradation with regard to transport, deposition, and erosion dynamics [11,17,24]. On the other hand, it was proven that single events, like floods, affect microplastic fluxes and that the variation in natural flow conditions causes variations in the transport behaviour of microplastics [17,24].

Despite the above findings discussed within former publications and recent reviews, it could be said that spatio-temporal considerations are, so far, rarely present in microplastic research [25]. With regard to microplastic fluxes in freshwater systems, so far, the spatial focus has been on first-order rivers, as well as sampling at different sites along a river [26]. Additionally, microplastic sampling has been performed mostly under moving conditions (net sampling from ships or boats) in a specific area of the river (e.g., central) with fixed depths [26,27]. With regard to temporal considerations, microplastics are often sampled on single days or over short times, not providing sufficient time series over longer durations (e.g., months, years) [28].

For example, a spatially detailed consideration of microplastic fluxes and particle properties in a river cross-section was able to demonstrate that (i) high-flow conditions affect lateral and vertical microplastic fluxes, (ii) river morphology affects microplastic fluxes, and (iii) storm events affect microplastic variety across a river section [27,29].

Given this context, the primary objective of our study was to quantify (micro)plastic loads based on a spatio-temporal sampling approach to provide further spatio-temporal data and gain further insights on the effects of natural flow variations on (micro)plastic transport behaviour in situ. In this study, we focused on (micro)plastics with a size range of 5000–500 µm, including single macroplastics (>5 mm). For this reason, we conducted our spatio-temporal stationary net sampling approach on the example of a single cross-section of Lahn River (second-order river, Central Germany). In order to reach our objective, we pursued the following research questions:

1. What microplastic loads are transported in the river under different flow conditions?
2. Are spatio-temporal variations in the microplastic loads and particle properties detectable?

3. Does the discharge affect the microplastic loads as well as the vertical and lateral transport behaviour?

2. Materials and Methods

2.1. Study Area

Sampling of macro- and microplastics from freshwater was conducted on the Lahn River (Germany). The Lahn River, with a total river length of 235.6 km, drains a catchment area of 5924 km^2 [30]. As a medium-sized secondary river, the Lahn River is one of the typical drainage systems within Central European low-mountain regions, comparable to many others in Central Europe. Spatio-temporal sampling was conducted at a single river cross-section (50.755487 N, 8.744362 E) located in the upper middle reaches (66.6 km after the spring) of the Lahn River. While the upper reaches of the Lahn River are rather rural-shaped, the investigated river cross-section is located 6 km downstream of the inner-city area of Marburg (approx. 75,000 inhabitants) and 1.5 km downstream of the sewage treatment plant Marburg–Cappel [30]. The direct surroundings of the cross-transect are dominated by pastures as flood water retention areas to the east and a gravel pit and a federal road (B3) to the west and land use shows a mixture of rural to slightly urbanized zones, from forests to arable land and artificial grounds (Figure 1). With regard to (micro)plastic inputs to the freshwater system within the drained catchment of the Lahn River, diffuse emissions from agriculture, infrastructure, and smaller urban areas, as well as villages, are likely [31]. The drained catchment area in question includes 74 municipal wastewater treatment plants (5 treatment plants >10,000 inhabitants; 17 treatment plants >2000 inhabitants), which represent a variety of potential additional point sources [30,32].

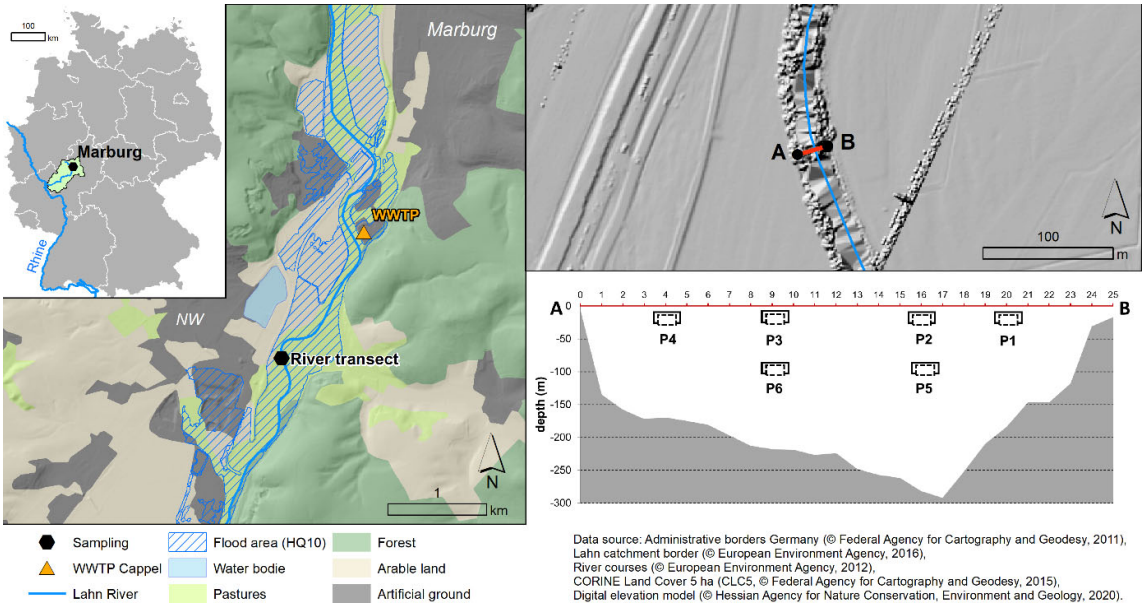

Figure 1. Top left: General map of the location of the study area in Germany: **left**—location of river cross-section and surrounding landscape features; **top right**—digital elevation model of river cross-section and surrounding floodplain with cut bank (**A**) and slip-off slope (**B**); and **bottom right**—river cross-section details with dimension, river morphology, and net sampling locations (P1–P6).

The sampled river cross-section is at a river bend between a cut bank (Figure 1, cross-section, point A) and a slip-off slope (Figure 1, cross-section point B), where the riverbed (active channel) shows a width of 25.0 m and a maximum depth of 2.92 m. The eastern side (B, slip-off) of the bank slopes relatively steeply, while the western side (A, cut bank) rises continuously (Figure 1 and Figure S1). The bank is covered with riparian woods (willows, alders), as well as reeds and cane, and is framed by pastures at the site. According to

the evaluation in the Water Framework Directive 2000/60/EC, the river section shows a strongly changed river structure [30].

2.2. Sampling

Spatio-temporal sampling was performed between 13 July 2020 and 22 March 2021, over 15 sampling dates. In order to perform stationary net sampling, a rope and tape measure were stretched across the river to ensure a continuous measurement. An inflatable boat served as a working platform (Figure S1). Sampling was performed at four positions at the water surface (P1–4) and two deeper positions (P5–6). A sampling net with a net inlet of 70 × 30 cm (0.28 m^2), a total length of 2.6 m, and a mesh size of 300 µm (microplastic net, Hydro-Bios Apparatebau GmbH, Altenholz, Germany) was used for sampling. Stationary sampling was then carried out for 45 min at each sampling position across the river cross-section by hanging the net from the boat into the water stream and attaching it to the rope in a stationary position (Figure S1). On 15 October and 16 October 2020, reference sampling with a duration of 6 h at a single position was conducted. With a sampling time of 45 min, the size of the net was sufficient, and clogging or filling with river loads (e.g., branches, leaves) was avoided. After the sampling time, the net was lifted and the contents of the net cup (collection cup, mesh size 300 µm, Hydro-Bios Apparatebau GmbH, Altenholz, Germany) were rinsed with river water in amber glass bottles (1 L). Afterwards, the net was placed in the river for 10 min without the collection cup for cleaning. With each sampling, the flow velocity (m/s) was measured simultaneously at the sites (P1–6) using a flow metre with an impeller (Z30, OTT HydroMet GmbH, Kempten, Germany).

2.3. Laboratory Analysis

The laboratory analysis included sample preparation (dehydration), size separation and filtration, staining, and identification. During laboratory analysis contamination prevention was ensured by avoiding plastic equipment, wearing cotton lab coats, and exclusively working with <50 µm filtered water.

To dehydrate the sample material and separate size fractions, the solid material was separated from the river water by sieving into size fractions >1000 µm and >500 µm (stainless-steel sieves, ø 75 mm, Atechnik GmbH, Leinburg, Germany) and rinsed using filtered (<50 µm) water. Due to the very low sediment load in the samples, the subsequential step of density separation was omitted [33,34]. The sieve residues were rinsed with demineralized water on pleated cellulose filter (600 P, ø 150 mm, Carl Roth GmbH, Karlsruhe, Germany). Filters were then transferred to glass Petri dishes and dried for 20 min at 50 °C in a closed drying chamber.

For the visual identification of potential MP particles, the residues were stained upon the cellulose filters with the help of a Nile Red solution. Nile Red staining procedures allow the identification of potential MP particles by fluorescence, as Nile Red adsorbs to polymeric surfaces [35,36]. Nile Red (Sigma-Aldrich, Taufkirchen, Germany) was dissolved to a concentration of 20 µg mL^{-1} within an ethanol–acetone (1:1) mixture following the suggestions of Konde et al. [35] and applied to the entire surface of the filters using a pipette and a spray bottle. Staining was then carried out for 10 min at 50 °C in a drying chamber [35]. Visual fluorescence identification was conducted afterwards under a stereomicroscope (SMZ 161 TL, Motic, Hong Kong) with a fluorescence setup (excitation: 465 nm LED; emissions: 530 nm colour long-pass filter; Thorlabs, Bergkirchen, Germany). Each fluorescent particle (often bright orange or yellow-greenish) was collected if its surface matched the criteria according to Noren [37]. Each potential plastic particles was stored within microplates (Brand, Wertheim, Germany), classified according to surface characteristics (shape, degradation, and colour), photographed (Moticam 2, Motic, Hong Kong), and their size measured (Motic Images Plus 3.0, Motic, Hong Kong).

In order to allow for polymer type identification and avoid the potential overestimation of organic residues with polymeric surfaces (e.g., freshwater shells), each collected particle was analyzed using a Tensor 37 FTIR spectrometer (Bruker Optics, Ettlingen, Germany)

combined with a Platinum-ATR-unit (Bruker Optics, Ettlingen, Germany). Measurements were conducted with a 20 background and sample scans with a spectral resolution of 4 cm^{-1} within a 4000 cm^{-1} to 400 cm^{-1} wavenumber range [38–40].

2.4. Statistics and Data Analysis

Basic data handling was performed within Microsoft Excel (version 1808, Microsoft, Redmond, WA, USA) or RStudio (version 1.3.1093, RStudio, Posit PBC, Boston, USA, 2020) within an R environment (version 4.0.3, R Core Team, Auckland, New Zealand, 2020). Statistical operations such as data visualization, *t*-test, linear regression models, Spearman rank correlations, and k-means clustering were performed within R. We used the R packages ggplot2 [41] and ggbubr [42] for data analysis and visualization. Significance was interpreted at the $p < 0.05$ level. Data relationships were interpreted as small with r^2 of 0.3–<0.5, medium with 0.5–<0.8, and strong ≥0.8.

Data processing of FTIR spectra was performed in OPUS 7.0 (Bruker Optics, Ettlingen, Germany) and Spectragryph (Version 1.2.14; [43]; Oberstdorf, Germany). Spectral identification was conducted within the available OPUS database (OPUS 7.0 internal database) and the OpenSpecy database [44]. Each identified spectrum with a hit ratio <700 (OPUS 7.0) was double-checked within the OpenSpecy database using full spectra, and Pearson's r with $r^2 > 0.6$ as a match quality indicator. A polymer type was then assigned to each plastic particle, and only particles definitely identified as polymers were counted as (micro)plastics.

Plastic loads were reported as plastic particle *p* (absolute plastic particle number) and plastic load (*PL*) in p m^3 (plastic particle per m^3 river water), calculated as follows (Equation (1)):

$$PL\left(\frac{p}{m^3}\right) = \frac{number\ of\ plastic\ particles\ (p)}{measured\ discharge\ (m^3)} \quad (1)$$

Discharge was calculated based on the measured flow rate (m s^{-1}) and related to the size of the net inlet (0.28 m^2) to obtain the discharge (m^3) per measurement period (45 min) given in m^3 s^{-1}.

In addition to the collected data (MP load and discharge in the river cross-section), local discharge data and regional precipitation data for the period July 2020 to April 2021 were used. Lahn River discharge data were retrieved for the Lahn gauge in Marburg (discharge in m^3 s^{-1}; gauge ID, 25830056; and river km, 175), which is 6 km upstream of the river cross-section and includes the upper Lahn catchment, with an area of 1666.2 km^2 [45]. Precipitation data were obtained for the period studied from the station "Cölbe" (daily precipitation sum in mm; station ID, DWD 3164), located 10.5 km to the north of the river cross-section [46].

The spatial interpolation of plastic loads (p m^3) and discharge (m^3) was conducted via Empirical Bayesian Kriging (EBK), without data transformations. EBK interpolation was carried out via the R packages "gstat" [47,48] and "raster" [49]. Final plots were created using the "levelplot" function from the "lattice" package [50].

Based on the data collected from the sampling points (P1–6, measured values) in the river cross-section, the intermediate spaces that could not be sampled were interpolated. Even though EBK is a satisfactory geostatistical method for interpolating spatially distributed data, limitations nevertheless arise [51]. Firstly, the measured values are a snapshot of the dynamic stream system, whose exact flow diversity can only be insufficiently captured on the basis of the existing data. However, we use EBK interpolation to spatially represent our data in a simple and quickly comprehensible way (no modelling but three-dimensional representation of the spatial data). The results of the EBK interpolation are not highly spatially representative, as the distribution of the sampling points is comparatively coarse for the EBK modelling quality. Interpolation was conducted for low-flow (day 7; 16 September 2020; and average Q = 58.97 m^3), medium-flow (day 1; 17 July 2020; and average Q = 69.55 m^3), and high-flow conditions (day 15; 22 March 2021; and average Q = 90.78 m^3), as well as for the total average from 15 measurement dates.

3. Results

3.1. Discharge Trends Across the River Section

Our sampling period, from 1 July 2020 to 1 April 2021, was characterized by a comparatively dry second half of 2020 and a change to wet conditions within the first months of 2021. Even though larger but short-term precipitation events (>20 mm) occurred regularly in the months from July to December 2021, the discharge of the Lahn River remained below the long-term average (MQ, gauge Marburg) (Figure 2). Regarding discharge data from the Lahn gauge Marburg, discharge of the Lahn River increased substantially in the sampling period only at the turn of the year 2020/2021 and showed typical sharply increasing discharge curves following precipitation events, with a delayed decrease in the discharge (Figure 2). The average discharge of the Lahn River at the gauge station in Marburg was 4.96 m^3 s^{-1} (July–December 2020), increasing to an average of 21.04 m^3 s^{-1} in January–April 2021.

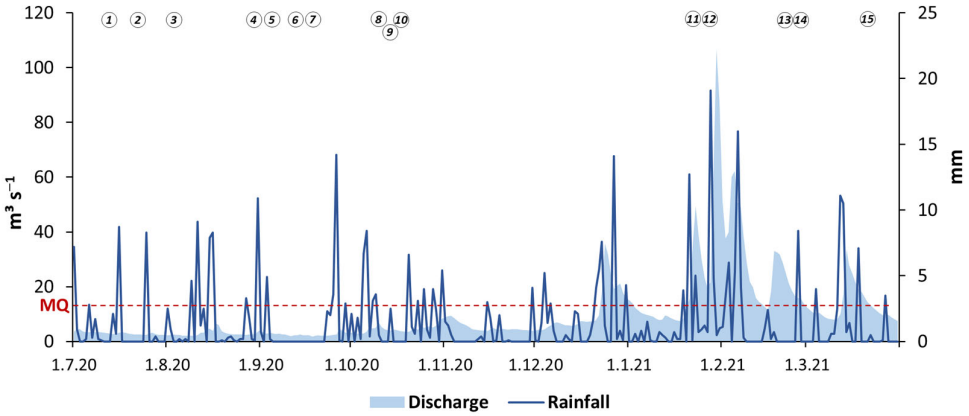

Figure 2. Daily averages of discharge and precipitation trends during the sampling period from July 2020 to April 2021. The sampling dates are numbered 1–15 (circles), and MQ indicates the long-term average discharge at the Lahn gauge. Discharge data source: Lahn gauge Marburg (gauge ID: 25830056). Rainfall data source: climate station Cölbe (station ID: DWD 3164).

In the river cross-section, the measured discharge (flow metre measurements) ranged from not measurable values (<5 m^3 s^{-1}) up to 116.3 m^3 s^{-1}, with a total average of 78.85 ± 19.01 m^3 s^{-1}, including fifteen measurement dates and all six sampling points across the river. During the dry period (July–December 2020), the average discharge within the river cross-section was 72.69 m^3 s^{-1} in the upper water column (sampling points 1–4) and 71.60 m^3 s−1 in the lower water column (sampling points 5–6). Within the wet period (January–April 2021), discharge increased, with average values of 91.62 m^3 s^{-1} in the upper and 92.61 m^3 s^{-1} in the lower water column. During the whole measurement period, discharge was higher at the slip-off slope (83.79 ± 19.88 m^3 s^{-1}) than at the cut bank (74.86 ± 17.28 m^3 s^{-1}).

3.2. (Mirco)plastic Loads and Characteristics

During 15 sampling campaigns, we found a total sum of 198 plastic particles (identified via ATR-FTIR) above our lower size detection limit of 500 µm. The sum of plastic particles sampled on each sampling date, including all net positions, ranged from 4 to 28 particles (average 13.20 ± 7.34 particles), over a total sampling time of 270 min or 4.5 h per day. Per sampling point (net position, P1–P6), the number of sampled plastic particles during 45 min of sampling ranged from 0 to 9 (average 2.75 ± 2.38 particles) (Table 1). Considering the whole sampling period, we found that, on average, 0.06 plastic particles per minute (p min^{-1}) or 3.67 plastic particles per hour (p h^{-1}), respectively, were sampled.

Table 1. Overview of (micro)plastic concentrations per sampling date, river cross-section position, and (micro)plastic size classes with measured discharge (Q) and microplastic loads (p m^3).

Date	Value [a]	MP Concentration and Discharge [b]						MP Concentration According to Size Classes			
		P1	P2	P3	P4	P5	P6	MP Sum/Day	MP Size Classes (µm)		
	x/*y*	20/0	16/0	9/0	4/0	16/−1	9/−1		>5000	>1000	>500
17 July 2020	p	0	4	3	1	1	0	9	3	4	2
	Q [c]	<5	83.2	68.0	68.0	76.0	52.9				
	p m^3	0	0.048	0.044	0.015	0.013	0				
22 July 2020	p	2	1	2	1	1	2	9	0	5	4
	Q	<5	75.6	60.5	52.9	75.6	60.5				
	p m^3	*	0.013	0.033	0.019	0.013	0.033				
3 August 2020	p	1	3	2	2	2	2	12	1	7	4
	Q	<5	75.6	60.5	68.0	60.5	60.0				
	p m^3	*	0.04	0.033	0.029	0.033	0.033				
1 September 2020	p	2	3	2	0	3	3	13	5	4	4
	Q	<5	105.8	98.3	75.6	98.3	75.6				
	p m^3	*	0.028	0.02	0	0.031	0.04				
3 September 2020	p	0	1	4	0	0	1	6	1	5	0
	Q	<5	75.6	60.5	52.9	75.6	52.9				
	v	*	0.013	0.066	0	0	0.019				
15 September 2020	p	2	1	0	0	2	0	5	0	3	2
	Q	<5	75.6	68.1	52.9	60.5	60.5				
	p m^3	*	0.013	0	0	0.033	0				
16 September 2020	p	1	0	0	0	3	2	6	2	3	1
	Q	<5	68.0	60.5	52.92	52.9	60.4				
	p/m^3	*	0	0	0	0.057	0.033				
13 October 2020	p	2	3	1	5	0	1	12	0	9	3
	Q	30.2	113.4	105.8	83.2	113.4	83.2				
	p m^3	0.066	0.026	0.009	0.06	0	0.012				
15 October 2020 6 h reference [d]	p	*	*	*	*	4	*	4	3	1	0
	Q	*	*	*	*	98.3	*				
	p m^3	*	*	*	*	0.005	*				
16 October 2020 6 h reference [d]	p	*	*	8	*	*	*	8	2	0	6
	Q	*	*	98.2	*	*	*				
	p m^3	*	*	0.01	*	*	*				
25 January 2021	p	6	6	5	4	*	*	21	10	8	3
	Q	90.2	116.3	108.1	97.1	*	*				
	p m^3	0.067	0.052	0.046	0.041	*	*				
26 January 2021	p	5	4	9	4	*	*	22	5	12	5
	Q	80.6	103.9	94.3	84.7	*	*				
	p m^3	0.062	0.038	0.095	0.047	*	*				
24 February 2021	p	7	7	9	5	*	*	28	8	12	8
	Q	79.7	108.6	100.3	85.9	*	*				
	p m^3	0.088	0.064	0.09	0.058	*	*				
25 February 2021	p	6	3	9	4	*	*	22	9	8	5
	Q	69.5	92.3	87.9	73.6	*	*				
	p m^3	0.086	0.033	0.107	0.054	*	*				
22 March 2021	p	3	7	2	4	2	3	21	2	11	8
	Q	73.4	106.3	98.1	81.6	95.4	89.9				
	p m^3	0.041	0.066	0.02	0.049	0.021	0.033				

[a] Measurement values: p, number of plastic particles per position (P1–P6); Q, discharge per position (P1–P6); and p/m^3, plastic particles per m^3 discharge. [b] Microplastic concentration and discharge per sampling position (P1–P6). [c] Average discharge (Q) per day. [d] Reference sampling (single position, stationary, duration: 6 h). * missing values (no measurement due to small or excessive discharge and flow load).

The calculated (micro)plastic loads ranged from 0.00 to 0.11 p m^3, with a total average of 0.03 ± 0.027 p m^3 over the whole sampling period, including all net positions (Table 1). The average (micro)plastic loads over 15 measurement dates for net positions P1–P6 ranged

between 0.03 and 0.06 p m^3 (P1 and P2, surface water, slip-off slope), 0.03–0.04 p m^3 (P3 and P4, surface water, cut bank), and around 0.02 p m^3 for deeper water (P5 and P6). The maximum (micro)plastic loads occurred at sampling point P3 (0.11 p m^3).

The sampled (micro)plastic particles consisted mainly of fragments, films, and filaments, with bright colours (e.g., red or blue) or white and transparent (Figure S2). With regard to plastic size classes, 25.7% could be attributed to the mesoplastic size class (>5000 µm). Within the microplastic size range, we found 46.5% of all particles to have a size between 5000 and 1000 µm and 27.8% to have a size between 1000 and 500 µm. Based on ATR-FTIR analysis and spectral identification, we found a clear dominance of polyethylene (PE), including high- and low-density PE, with a share of 71.93%, followed by polypropylene (PP) with a share of 20.18%, polystyrene (PS) with 7.02%, and polyamide (PA) with 0.88%.

3.3. Spatio-Temporal (Micro)plastic Variations

Meso- and microplastic abundance within the studied river cross-section varied between the sampling points (net positions, P1–P6) (Table 1). In general, the lowest (micro)plastic abundance was recorded in the deeper sampling positions (1 m below the water surface, P5–P6), with average particle numbers of 1.56 p (P6) and 1.80 p (P5) per 45 min of sampling. For deeper sampling points, average (micro)plastic loads of 0.022 p m^3 were calculated within average discharges of 73.81 ± 17.71 m^3 s^{-1}. In contrast, the average particle numbers increased at the cut bank site (P1–P2), with a total average of 3.08 ± 2.25 p, continuing to 3.19 ± 2.85 p at the slip-off slope site (P3–P4) per 45 min of sampling. In contrast, the (micro)plastic loads were slightly higher at the cut bank site (av.: 0.042 p m^3) than at the slip-off site (av.: 0.035 p m^3), because of the higher river discharge at the cut bank site, with 85.47 ± 20.17 m^3 s^{-1} compared to 77.73 ± 17.69 m^3 s^{-1} at the slip-off site.

In addition to these spatial variations in the river cross-section, temporal variations in meso- and microplastic abundance appeared. With regard to the general division of weather and discharge conditions within a dry period (low discharge) during the second half of 2020 and a wet period (high discharge) in the spring of 2021, the abundance of (micro)plastics changed significant over time (Figure 2). The daily sum of plastic particles changed significantly ($p < 0.01$, *t*-test) under wet conditions, up until January 2021, with an average of 8.4 particles over 10 sampling campaigns in 2020 and an average of 22.8 particles over 5 sampling campaigns in 2021. The daily average of (micro)plastic loads also changed significantly ($p < 0.01$, *t*-test), similarly to the discharge conditions and number of sampled plastic particles, with the turn of the year 2020/21, from 0.02 to 0.06 p m^3.

Comparing (micro)plastic abundance with self-measured site-specific discharge across all sampling points (P1–P6) and for all 15 sampling dates, we found a clear evidence (ANOVA $p < 0.05$) that higher plastic abundances (av.: 22.8 p) occurred under high-flow (>10 m^3 s^{-1}) conditions than under medium- (>4 m s^{-1}) or low-flow (<4 m^3 s^{-1}) conditions (Figure 3). Furthermore, comparing (micro)plastic abundance with superordinate discharge measurements at the Marburg gauge (Figure 3), we found a linear relationship ($R^2 = 0.71$) between discharge and (micro)plastic abundance, characterized by the division of values into two classes (discharge conditions: low vs. high) (Figure 4). With regard to the differentiated plastic size classes (>5000 µm meso-, >1000 µm large- micro-, and >500 µm microplastics) during plastic analysis, we found decreasing linear relationships with decreasing particle sizes (Figure 4b–d).

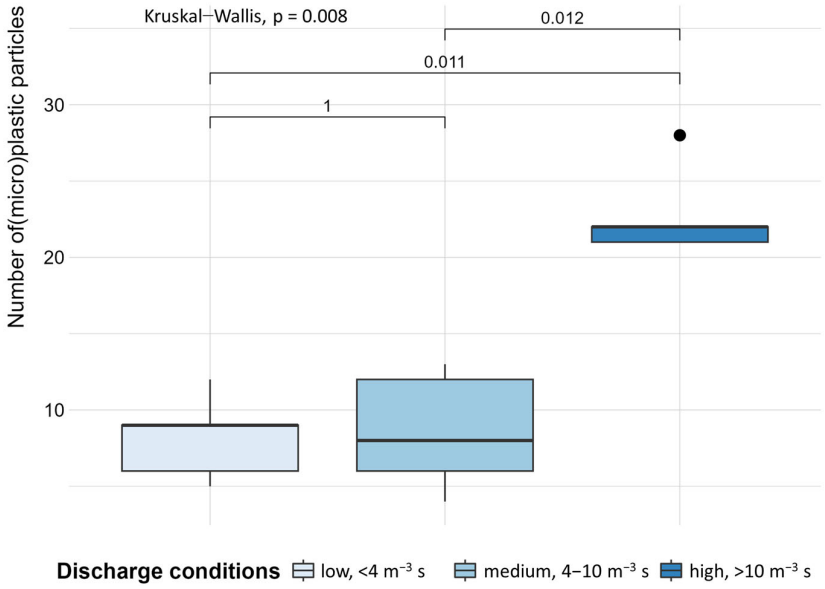

Figure 3. Number of identified (micro)plastic particles under different discharge conditions, classified according to low flow (<4 m^3 s^{-1}), medium flow (4–10 m^3 s^{-1}), and high flow (>10 m^3 s^{-1}) at different sampling points. Mean comparisons via Kruskal–Wallis test.

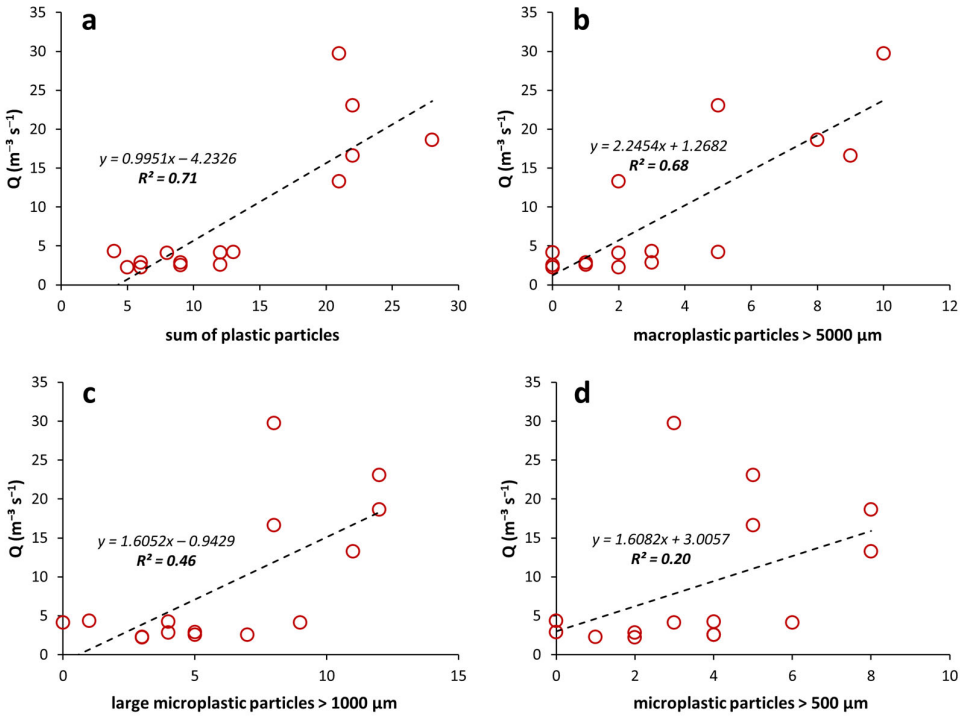

Figure 4. Linear regressions between discharge (Q, m^3 s^{-1}) and (micro)plastic particles classified according to size classes (**a**) sum, (**b**) >5000 µm, (**c**) >1000 µm, (**d**) and >500 µm).

The overall Spearman correlation between the sum of (micro)plastic particles per day and the superordinate discharge data from gauge Marburg appeared to have a significant correlation (RSP: 0.52, $p < 0.05$), indicating a medium positive relationship between (micro)plastic abundance and discharge conditions within the river.

Beyond the consideration of meso- and microplastic abundance, spatio-temporal variations in plastic characteristics became apparent as well. With regard to plastic particle size classes, we found a dominance of particles with a size between 5000 and 1000 µm (48.8% in 2020, 44.7% in 2021) under both low- and high-flow conditions. During the

low-flow conditions in 2020, smaller particles (1000–500 µm) occurred more frequently (31.0%) than mesoplastics (>5000 µm), measuring 20.2%. These proportions changed under high-flow conditions in 2021, during which mesoplastics accounted for a larger share (29.8%) than microplastics (25.4%).

While no spatio-temporal variations were found for particle shapes and colours, spatial differences in polymer type distribution were present (Figure 5). Briefly, we identified a dominance of polyethylene (both HDPE and LDPE) at the upper sampling points, including the cut bank and the slip-off section. In contrast, limited by the generally lower plastic abundance in deeper samples (P5–P6), we found a dominance of PE and PS at point P6 and a dominance of PE and PP in the absence of PS at point P5.

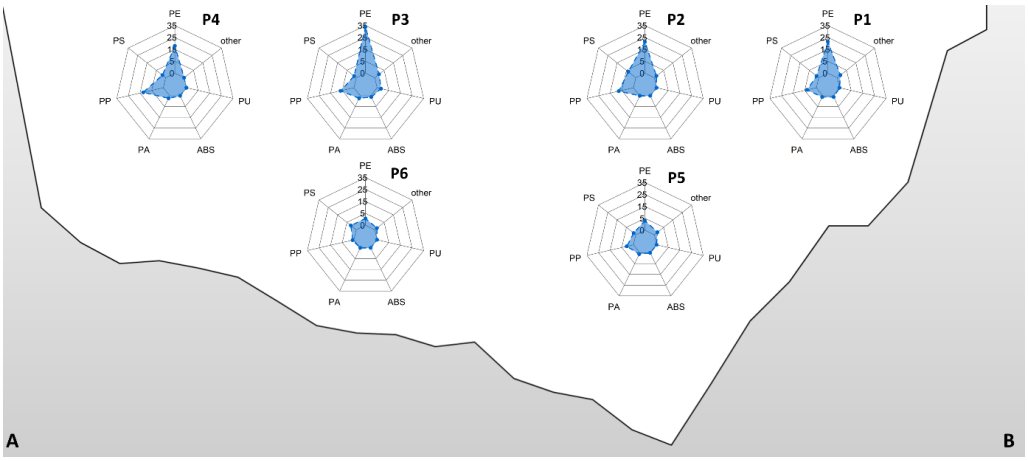

Figure 5. Polymer type occurrence at sampling points within river cross-section with (**A**) cut bank and (**B**) slip-off slope.

3.4. Spatial Interpolation of (Micro)plastic Loads Across the River

The spatial interpolation over the entire river cross-section based on the collected point data illustrated the spatio-temporal variations in (micro)plastic abundance and river discharge (Figure 6). With regard to the entire sampling period, including all 15 measurement dates, we found a higher presence of (micro)plastics near the shore at the slip-off site and a continuous decrease towards the opposite cut bank side, while major flow occurred within the central river, with a slight tendency towards the slip-off side (Figure 6a). Great (micro)plastics loads shifted towards the center of the river under low-flow conditions (Figure 6b), shifting backwards towards the slip-off slide under medium-flow conditions (Figure 6c), occurring on both sides of the river but with a stronger expression on the slip-off side under high-flow conditions (Figure 6d). In contrast, the interpolated flow conditions showed major flow at the cut bank site during low- and medium-flow conditions (Figure 6b,c), while major flows were recorded towards the center of the river under high-flow conditions (Figure 6d). In comparison, many (micro)plastics and, therefore, higher plastic loads occurred primarily in transitional areas between high- and low-flow conditions across the river section.

A further data evaluation independent of the spatial interpolation showed that the largest data range of both plastic abundance and discharge occurred at the slip-off slope site, while more constant (micro) plastic loads and discharge conditions occurred at the cut bank site (Figure 7a). Additionally, within deeper water sections, we identified constant discharge conditions but also, more frequently, zero values of plastic abundance. A cluster analysis (k-means) of the whole (micro)plastic loads and discharge dataset identified three clusters (Figure 7b). Cluster one included medium-discharge conditions and medium (micro)plastic loads, whereas cluster two included high-discharge conditions and the highest (micro)plastic loads, representing an expression of the already described dependencies between discharge and plastic loads. Additionally, cluster three included single data points with low-discharge conditions and the lowest (micro)plastic loads. In comparison, it is

therefore evident that a tendency for the clustering to be dependent on the discharge conditions and not on the location within the river cross-section was expressed by the cluster analysis, with the exception of the third cluster including only slip-off slope data.

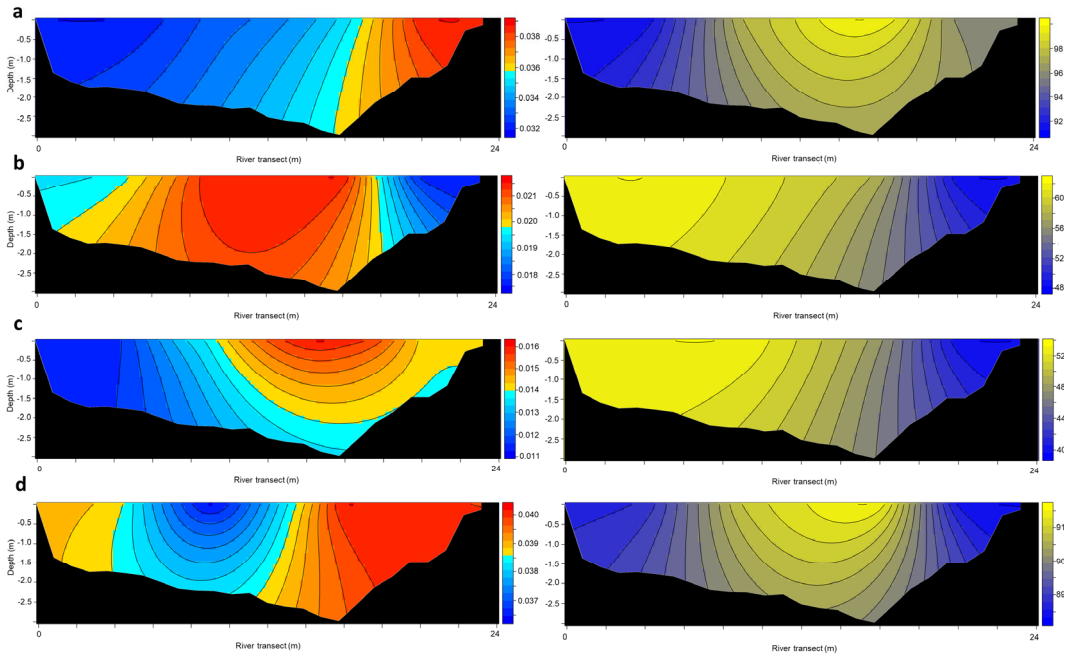

Figure 6. Spatial interpolation within the river cross-section of plastic loads (p m^3, **left**) and discharge (m^3 s^{-1}, **right**) under different discharge conditions. (**a**) Total average from 15 measurement dates; (**b**) low-flow conditions (day 7; 16 September 2020; average Q = 58.97 m^3 s^{-1}); (**c**) medium-flow (day 1; 17 July 2020; average Q = 69.55 m^3 s^{-1}); and (**d**) high-flow conditions (day 15; 22 March 2021; average Q = 90.78 m^3 s^{-1}).

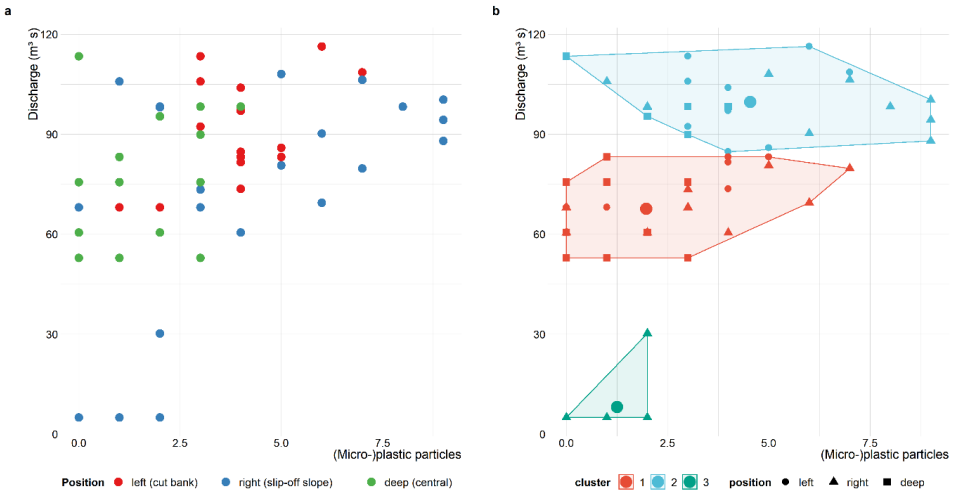

Figure 7. Comparison of (micro)plastic particle abundance with sampling discharge conditions (field measurements): (**a**) (micro)plastic particle abundance compared to discharge at sampling points grouped according to sampling point locations on the left (cut bank, P3–P4), right (slip-off slope, P1–P2), and in the depths (deeper samples, P5–P6); and (**b**) results of k-means clustering of (micro)plastic particle abundance and discharge data grouped according to three major data clusters and sampling point locations, by (**a**) shape.

4. Discussion

The sampling period from 1 July 2020 to 1 April 2021 covered all discharge conditions occurring within the Lahn River, ranging from low- to high-discharge conditions, with

dry-weather discharge lasting well into the autumn of the year 2020. Such dry conditions combined with a low flow have occurred very often in recent years and indicate the effects of climate change on hydrological conditions.

These different discharge conditions are also reflected in the transport of microplastics. A total of 198 particles were found, which, distributed over the entire sampling period, accounted for an average temporal distribution of 3.67 plastic particles per hour (p h^{-1}). This resulted in an average microplastic load of 0.03 ± 0.027 p m^3. For rivers of a similar size to the Lahn River, there are hardly any data on loads and concentrations, which is why it is difficult to classify the results regarding microplastic loads obtained in this study. Studies on larger rivers (e.g., [14,16,52]) with significantly more anthropogenic sources of microplastics show correspondingly higher loads. For example, ref. [27] reported a load of 2.57 p/m^3 for the Hillsborough River, which has a catchment area of 984 km^2, also indicating a higher concentration of 1.35–2.71 p m^3. When considering data on microplastic loads in rivers, it is important to note that different methods of data collection already lead to different results. While the nets used in [16,23,24] had a mesh size of 55 µm (plankton net (nylon)) and 80 µm, respectively, those in [27,29,52,53] were between 300 and 500 µm. Refs. [15,22] did not give any information on the mesh size. In this study, a net with a mesh size of 300 µm was applied, and, therefore, we were not able to consider plastic particles smaller than this size. Thus, micro- and nanoplastic particles could not be considered.

Within the studied river cross-section (Lahn River), meso- and microplastic abundance varied between the sampling points (net positions, P1-P6) (Table 1). In general, the lowest (micro)plastic abundance was recorded within the deeper sampling positions (1 m below the water surface, P5–P6), with average particle numbers of 1.56 p (P6) and 1.80 p (P5) per 45 min of sampling. Our results regarding depth distribution are similar to those of [25] who also found that most plastic particles are transported close to the water surface. A smaller fraction of plastics mixes deeper into the water column, where it may accumulate within the river system, gradually degrading and intermittently being reintroduced into the flow.

The above results are also in line with the study of [29], which stated that most of the plastic transported in the Mekong River was found on the surface, while a smaller portion was mixed deep into the water column. Many of the studies on microplastic loads in rivers only measured at one depth, usually near the water surface (e.g., [54]), so only part of the total microplastic load was recorded [27]. Many of these studies also took plastic samples at several points along a river cross-section and at several depths (Hillsborough River), similar to this study, and were able to determine a spatial distribution across the river cross-section. As in our study, the higher loads were found on the cut bank, while the concentrations were lower on the slip-off side.

With regard to the role of hydrology on the transport of microplastics, there is a clear link between runoff and the microplastic load in the Lahn River expressed by ANOVA, linear relationships, and Spearman correlations. There is clear evidence that higher plastic abundances (av.: 22.8 p) occur under high-flow (>10 m^3 s^{-1}) conditions than under medium- (>4 m s^{-1}) or low-flow (<4 m^3 s^{-1}) conditions. This is in accordance with the results of [24,27,29], who also found that storm events led to both the dilution and intensification of plastic pollution. Ref. [27] underlined that, during high-flow conditions, lateral and vertical fluxes became important transport mechanisms in their research. Despite these clear correlations, the question is whether higher discharges transport additionally microplastics that enter the river from various sources (e.g., surface runoff from roads) or whether it is plastic stored in the river system that is reactivated and transported by the hydraulic turbulence. It should also be noted that, if only the smaller particles are considered, the influence of runoff on transport is somewhat reduced. So far, little is known or has been determined in detail about the residence times of plastics in open rivers or urban terrestrial environments [27]. In principle, some plastics may spend a long time in the terrestrial environment before being displaced into the river via lateral exchange processes. Some microplastics are deposited in river sediments during low-flow conditions and are

reactivated at higher flows [55]. However, these findings are only based on a comparison of microplastic particle abundances in river sediments between low-flow and high-flow conditions. Small-scale differences in microplastic load in river sediments at the time of sampling could lead to misinterpretations. Ref. [56] developed a theoretical model of plastic transport in rivers and considered remobilisation in sediments; however, such models have not yet been validated, so further experimental studies in the field are essential to better assess the dynamics of the sediment water column with respect to microplastic transport. If we look more closely at the linear relationship between microplastic transport and runoff, we see from studies on the Lahn River that smaller particles tend to be transported independently of the runoff. Higher concentrations can also occur at lower discharges. The reasons for this are largely unclear, as there is also a lack of comparative studies. Ref. [27], therefore, calls for further studies that focus on identifying the size and shape of microplastics in order to understand the transport mechanisms and improve model predictions.

5. Conclusions

For this study on the Lahn River, a comprehensive dataset of river flows and plastic particles has been collected and analyzed to investigate the transport mechanisms in a river cross-section of a typical low-mountain river. There is a tendency for most microplastics to be transported to the surface of the water column. The distribution in the cross-section showed that the concentrations and loads were higher on the cut bank than on the slip-off slope, which was due to the different flow velocity in the cross-section. In general, if discharges increased, the number of plastic particles increased. This linear relationship applied mainly to the larger particles; for the smaller particles, this relationship was rather weak. However, the question remains open as to where the microplastics occurring at higher discharges come from. Increased loads from additional source areas or the remobilisation of particles from river sediments are possible causes. Overall, this study shows that the transport of plastics in rivers is uneven across a river cross-section and strongly depends on the hydrodynamic cross-section profile and the hydrological conditions. Such detailed studies on the transport of microplastics in rivers are still necessary to validate model assumptions and better understand the transport mechanisms, especially the reactivation of microplastics from sediments.

Supplementary Materials: The following supporting information can be downloaded at https://www.mdpi.com/article/10.3390/microplastics3040047/s1: Figure S1: An inflatable boat served as a working platform; Figure S2: The sampled (micro)plastic particles.

Author Contributions: Conceptualization, P.C. and C.J.W.; methodology, C.J.W.; validation, C.J.W.; formal analyses, T.N. and C.J.W.; investigation, T.N. and C.J.W.; resources, P.C.; data curation, T.N. and C.J.W.; writing—original draft, P.C. and C.J.W.; writing—review and editing, P.C., T.N. and C.J.W.; visualization, C.J.W.; supervision, P.C.; and project administration, P.C. and C.J.W. All authors have read and agreed to the published version of the manuscript.

Funding: Open Access funding provided by the Open Access Publishing Fund of Philipps-Universität Marburg.

Institutional Review Board Statement: Not applicable.

Informed Consent Statement: Not applicable.

Data Availability Statement: Data generated within the framework of this study can be downloaded at datadryad (https://datadryad.org/stash/share/uaoGB_NTc59VI1hFYrpP3XPPJPdFP2-YT-rwMUU34MA), accessed on 5 December 2024.

Acknowledgments: We would like to express our sincere gratitude to Olga Schechtel for her meticulous laboratory analyses and to Petrina Schick for her dedicated preparation of the water samples. Their expertise and hard work were invaluable in the successful completion of this study.

Conflicts of Interest: Author Thorsten Nather was employed by the company Engineering Office Greiwe and Helfmeier. The remaining authors declare that the research was conducted in the absence of any commercial or financial relationships that could be construed as a potential conflict of interest.

References

1. Syberg, K.; Nielsen, M.B.; Oturai, N.B.; Clausen, L.P.W.; Ramos, T.M.; Hansen, S.F. Circular economy and reduction of micro(nano)plastics contamination. *J. Hazard. Mater. Adv.* **2022**, *5*, 100044. [CrossRef]
2. Andrady, A.L. The plastic in microplastics: A review. *Mar. Pollut. Bull.* **2017**, *119*, 12–22. [CrossRef] [PubMed]
3. Hartmann, N.B.; Hüffer, T.; Thompson, R.C.; Hassellöv, M.; Verschoor, A.; Daugaard, A.E.; Rist, S.; Karlsson, T.; Brennholt, N.; Cole, M.; et al. Are We Speaking the Same Language? Recommendations for a Definition and Categorization Framework for Plastic Debris. *Environ. Sci. Technol.* **2019**, *53*, 1039–1047. [CrossRef] [PubMed]
4. *ISO/TR 21960:2020(en)*; Plastics—Environmental Aspects—State of Knowledge and Methodologies. International Organization for Standardization: Geneva, Switzerland, 2020. Available online: https://www.iso.org/obp/ui/#iso:std:iso:tr:21960:ed-1:v1:en (accessed on 1 February 2022).
5. Silva, A.B.; Bastos, A.S.; Justino, C.I.L.; Da Costa, J.P.; Duarte, A.C.; Rocha-Santos, T.A.P. Microplastics in the environment: Challenges in analytical chemistry—A review. *Anal. Chim. Acta* **2018**, *1017*, 1–19. [CrossRef] [PubMed]
6. PlasticsEurope. Plastics—The Facts 2021: An Analysis of European Plastic Production, Demand and Waste Data. Available online: https://plasticseurope.org/knowledge-hub/plastics-the-facts-2021/ (accessed on 1 February 2023).
7. Barnes, D.K.A.; Galgani, F.; Thompson, R.C.; Barlaz, M. Accumulation and fragmentation of plastic debris in global environments. *Philos. Trans. R. Soc. Lond. B Biol. Sci.* **2009**, *364*, 1985–1998. [CrossRef]
8. Chamas, A.; Moon, H.; Zheng, J.; Qiu, Y.; Tabassum, T.; Jang, J.H.; Abu-Omar, M.; Scott, S.L.; Suh, S. Degradation Rates of Plastics in the Environment. *ACS Sustain. Chem. Eng.* **2020**, *8*, 3494–3511. [CrossRef]
9. Chen, Y.; Awasthi, A.K.; Wei, F.; Tan, Q.; Li, J. Single-use plastics: Production, usage, disposal, and adverse impacts. *Sci. Total Environ.* **2021**, *752*, 141772. [CrossRef]
10. Lechthaler, S.; Waldschläger, K.; Stauch, G.; Schüttrumpf, H. The Way of Macroplastic through the Environment. *Environments* **2020**, *7*, 73. [CrossRef]
11. He, B.; Smith, M.; Egodawatta, P.; Ayoko, G.A.; Rintoul, L.; Goonetilleke, A. Dispersal and transport of microplastics in river sediments. *Environ. Pollut.* **2021**, *279*, 116884. [CrossRef]
12. Hüffer, T.; Praetorius, A.; Wagner, S.; von der Kammer, F.; Hofmann, T. Microplastic Exposure Assessment in Aquatic Environments: Learning from Similarities and Differences to Engineered Nanoparticles. *Environ. Sci. Technol.* **2017**, *51*, 2499–2507. [CrossRef]
13. Lebreton, L.C.M.; van der Zwet, J.; Damsteeg, J.-W.; Slat, B.; Andrady, A.; Reisser, J. River plastic emissions to the world's oceans. *Nat. Commun.* **2017**, *8*, 15611. [CrossRef] [PubMed]
14. Fan, J.; Zou, L.; Zhao, G. Microplastic abundance, distribution, and composition in the surface water and sediments of the Yangtze River along Chongqing City, China. *J. Soils Sediments* **2021**, *21*, 1840–1851. [CrossRef]
15. Kiss, T.; Fórián, S.; Szatmári, G.; Sipos, G. Spatial distribution of microplastics in the fluvial sediments of a transboundary river—A case study of the Tisza River in Central Europe. *Sci. Total Environ.* **2021**, *785*, 147306. [CrossRef] [PubMed]
16. Sekudewicz, I.; Dąbrowska, A.M.; Syczewski, M.D. Microplastic pollution in surface water and sediments in the urban section of the Vistula River (Poland). *Sci. Total Environ.* **2021**, *762*, 143111. [CrossRef]
17. Hurley, R.; Woodward, J.; Rothwell, J.J. Microplastic contamination of river beds significantly reduced by catchment-wide flooding. *Nat. Geosci.* **2018**, *11*, 251–257. [CrossRef]
18. Klein, S.; Worch, E.; Knepper, T.P. Occurrence and Spatial Distribution of Microplastics in River Shore Sediments of the Rhine-Main Area in Germany. *Environ. Sci. Technol.* **2015**, *49*, 6070–6076. [CrossRef]
19. Blettler, M.C.M.; Ulla, M.A.; Rabuffetti, A.P.; Garello, N. Plastic pollution in freshwater ecosystems: Macro-, meso-, and microplastic debris in a floodplain lake. *Environ. Monit. Assess.* **2017**, *189*, 581. [CrossRef]
20. Horton, A.A.; Dixon, S.J. Microplastics: An introduction to environmental transport processes. *WIREs Water* **2018**, *5*, e1268. [CrossRef]
21. Ballent, A.; Purser, A.; de Jesus Mendes, P.; Pando, S.; Thomsen, L. Physical transport properties of marine microplastic pollution. *Biogeosci. Discuss.* **2012**, *9*, 18755–18798.
22. Alam, F.C.; Sembiring, E.; Muntalif, B.S.; Suendo, V. Microplastic distribution in surface water and sediment river around slum and industrial area (case study: Ciwalengke River, Majalaya district, Indonesia). *Chemosphere* **2019**, *224*, 637–645. [CrossRef]
23. Bujaczek, T.; Kolter, S.; Locky, D.; Ross, M.S. Characterization of microplastics and anthropogenic fibers in surface waters of the North Saskatchewan River, Alberta, Canada. *Facets* **2021**, *6*, 26–43. [CrossRef]
24. Treilles, R.; Gasperi, J.; Tramoy, R.; Dris, R.; Gallard, A.; Partibane, C.; Tassin, B. Microplastic and microfiber fluxes in the Seine River: Flood events versus dry periods. *Sci. Total Environ.* **2022**, *805*, 150123. [CrossRef] [PubMed]
25. Kukkola, A.; Runkel, R.L.; Schneidewind, U.; Murphy, S.F.; Kelleher, L.; Sambrook Smith, G.H.; Nel, H.A.; Lynch, I.; Krause, S. Prevailing impacts of river management on microplastic transport in contrasting US streams: Rethinking global microplastic flux estimations. *Water Res.* **2023**, *240*, 120112. [CrossRef] [PubMed]

26. Stock, F.; Kochleus, C.; Bänsch-Baltruschat, B.; Brennholt, N.; Reifferscheid, G. Sampling techniques and preparation methods for microplastic analyses in the aquatic environment—A review. *TrAC Trends Anal. Chem.* **2019**, *113*, 84–92. [CrossRef]
27. Haberstroh, C.J.; Arias, M.E.; Yin, Z.; Sok, T.; Wang, M.C. Plastic transport in a complex confluence of the Mekong River in Cambodia. *Environ. Res. Lett.* **2021**, *16*, 95009. [CrossRef]
28. Metz, T.; Koch, M.; Lenz, P. Quantification of microplastics: Which parameters are essential for a reliable inter-study comparison? *Mar. Pollut. Bull.* **2020**, *157*, 111330. [CrossRef]
29. Haberstroh, C.J.; Arias, M.E.; Yin, Z.; Wang, M.C. Effects of hydrodynamics on the cross-sectional distribution and transport of plastic in an urban coastal river. *Water Environ. Res.* **2021**, *93*, 186–200. [CrossRef]
30. Hessisches Landesamt für Naturschutz, Umwelt und Geologie. WRRL-Viewer. Available online: https://wrrl.hessen.de (accessed on 1 February 2019).
31. Hessian State Office of Statistics. Hessische Gemeindestatistik—Gemeinden in Hessen (Hessian Municipal Statistics—Municipalities in Hesse). Available online: https://statistik.hessen.de/publikationen/hessische-gemeindestatistik (accessed on 1 February 2023). (In German).
32. Regional Council Giessen. *Hochwasserrisikomanagementplan für das Hessische Einzugsgebiet der Lahn (Flood Risk Management Plan)*; Regional Council Giessen: Giessen, Germany, 2015. Available online: https://www.hlnug.de/fileadmin/dokumente/wasser/hochwasser/hwrmp/Lahn/Erlaeuterungsbericht-HWRM-Lahn.pdf (accessed on 1 February 2023).
33. Hidalgo-Ruz, V.; Gutow, L.; Thompson, R.C.; Thiel, M. Microplastics in the marine environment: A review of the methods used for identification and quantification. *Environ. Sci. Technol.* **2012**, *46*, 3060–3075. [CrossRef]
34. Hurley, R.R.; Lusher, A.L.; Olsen, M.; Nizzetto, L. Validation of a Method for Extracting Microplastics from Complex, Organic-Rich, Environmental Matrices. *Environ. Sci. Technol.* **2018**, *52*, 7409–7417. [CrossRef]
35. Konde, S.; Ornik, J.; Prume, J.A.; Taiber, J.; Koch, M. Exploring the potential of photoluminescence spectroscopy in combination with Nile Red staining for microplastic detection. *Mar. Pollut. Bull.* **2020**, *159*, 111475. [CrossRef]
36. Maes, T.; Jessop, R.; Wellner, N.; Haupt, K.; Mayes, A.G. A rapid-screening approach to detect and quantify microplastics based on fluorescent tagging with Nile Red. *Sci. Rep.* **2017**, *7*, 44501. [CrossRef] [PubMed]
37. Noren, F. Small Plastic Particles in Coastal Swedish Waters. N. Research Report commissioned by KIMO Sweden, Göteborg. 2007. Available online: https://www.researchgate.net/publication/284312290_Small_plastic_particles_in_Coastal_Swedish_waters#fullTextFileContent (accessed on 11 February 2023).
38. Jung, M.R.; Horgen, F.D.; Orski, S.V.; Rodriguez C., V.; Beers, K.L.; Balazs, G.H.; Jones, T.T.; Work, T.M.; Brignac, K.C.; Royer, S.-J.; et al. Validation of ATR FT-IR to identify polymers of plastic marine debris, including those ingested by marine organisms. *Mar. Pollut. Bull.* **2018**, *127*, 704–716. [CrossRef] [PubMed]
39. Primpke, S.; Lorenz, C.; Rascher-Friesenhausen, R.; Gerdts, G. An automated approach for microplastics analysis using focal plane array (FPA) FTIR microscopy and image analysis. *Anal. Methods* **2017**, *9*, 1499–1511. [CrossRef]
40. Primpke, S.; Wirth, M.; Lorenz, C.; Gerdts, G. Reference database design for the automated analysis of microplastic samples based on Fourier transform infrared (FTIR) spectroscopy. *Anal. Bioanal. Chem.* **2018**, *410*, 5131–5141. [CrossRef] [PubMed]
41. Wickham, H. Getting Started with ggplot2. In *ggplot2. Use R!* Springer: Cham, Switzerland, 2016.
42. Kassambara, A. ggpubr: 'ggplot2' Based Publication Ready Plots. 2023. Available online: https://rpkgs.datanovia.com/ggpubr/ (accessed on 21 September 2023).
43. Menges, F. *Spectragryph Optical Spectroscopy Software*; Version 1.2. 14; Dr. Friedrich Menges Software-Entwicklung: Oberstdorf, Germany, 2019.
44. Cowger, W.; Steinmetz, Z.; Gray, A.; Munno, K.; Lynch, J.; Hapich, H.; Primpke, S.; de Frond, H.; Rochman, C.; Herodotou, O. Microplastic Spectral Classification Needs an Open Source Community: Open Specy to the Rescue! *Anal. Chem.* **2021**, *93*, 7543–7548. [CrossRef]
45. Hessian Agency for Nature Conservation, Environment and Geology. Discharge Data Station: Marburg (25830056). Available online: https://www.hlnug.de/static/pegel/wiskiweb2/# (accessed on 1 February 2023).
46. Hessian Agency for Nature Conservation, Environment and Geology. Wetterextreme Hessen (Weather and Climate Data Hesse). Available online: https://www.hlnug.de/themen/wasser/niederschlag#c61782 (accessed on 1 February 2023). (In German)
47. Gräler, B.; Pebesma, E.; Heuvelink, G. Spatio-Temporal Interpolation using gstat. *R J.* **2016**, *8*, 204. [CrossRef]
48. Pebesma, E.J. Multivariable geostatistics in S: The gstat package. *Comput. Geosci.* **2004**, *30*, 683–691. [CrossRef]
49. Hijmans, R.J.; Van Etten, J.; Cheng, J.; Mattiuzzi, M.; Sumner, M.; Greenberg, J.A.; Lamigueiro, O.P.; Bevan, A.; Racine, E.B.; Shortridge, A. Package 'raster'. R Package. 2022. Available online: https://CRAN.R-project.org/package=raster (accessed on 1 February 2023).
50. Sarkar, D. *Lattice: Multivariate Data Visualization with R*, 1st ed.; Springer: New York, NY, USA, 2008; ISBN 9780387759685.
51. GIS Geography. *Kriging Interpolation—The Prediction Is Strong in this One*; GIS Geography: Abbeville, LA, USA, 2022.
52. Wong, J.K.H.; Lee, K.K.; Tang, K.H.D.; Yap, P.-S. Microplastics in the freshwater and terrestrial environments: Prevalence, fates, impacts and sustainable solutions. *Sci. Total Environ.* **2020**, *719*, 137512. [CrossRef]
53. Frank, Y.A.; Vorobiev, D.S.; Kayler, O.A.; Vorobiev, E.D.; Kulinicheva, K.S.; Trifonov, A.A.; Soliman Hunter, T. Evidence for Microplastics Contamination of the Remote Tributary of the Yenisei River, Siberia—The Pilot Study Results. *Water* **2021**, *13*, 3248. [CrossRef]
54. Mani, T.; Hauk, A.; Walter, U.; Burkhardt-Holm, P. Microplastics profile along the Rhine River. *Sci. Rep.* **2015**, *5*, 17988. [CrossRef]

55. Xia, F.; Yao, Q.; Zhang, J.; Wang, D. Effects of seasonal variation and resuspension on microplastics in river sediments. *Environ. Pollut.* **2021**, *286*, 117403. [CrossRef]
56. Nizzetto, L.; Bussi, G.; Futter, M.N.; Butterfield, D.; Whitehead, P.G. A theoretical assessment of microplastic transport in river catchments and their retention by soils and river sediments. *Environ. Sci. Process. Impacts* **2016**, *18*, 1050–1059. [CrossRef]